The relationship between size, abundance, and mass of particles in the surface and bottom waters of the Chesapeake Bay

Emily Dougherty[1], Jacob Cram[1], and Ashley Hollins[1]

[1]University of Maryland Center for Environmental Science

November 21, 2022

Abstract

Particulate matter modulates the transport of carbon and nutrients through estuarine environments. In the Chesapeake Bay, sinking of particles and their consumption by microbes likely modulates the emergence of a seasonal oxygen deficient zone. The relationship between particle size and abundance affects the transport dynamics of the particles and the biology of associated organisms. The variability of particle characteristics has not previously been characterized across the length of the Chesapeake Bay, nor has it been compared to the oxygen deficient zone. Therefore, we measured the size to mass and size to abundance relationship of suspended particles along the Chesapeake Bay during a major deoxygenation event. A laser scattering instrument measured particle size and abundance at six stations. Five particle size classes were sampled at surface and bottom depths. Particles in the less saline northern end of the Bay were less massive relative to size than particles farther south. Estimates of total particle mass, calculated by combining particle size to mass and particle size to abundance data, suggested that the anoxic region has lower particulate mass than overlying oxic water, perhaps because stratified water above the oxygen minimum zone keeps particles from the productive top layer from mixing into this region. Total particle mass was higher just above the sediment, suggesting resuspension of benthic particles. Our data provide the first systematic survey of size resolved particle abundances across the Chesapeake Bay oxygen minimum zone and provide context to future work in evaluating the biogeochemical role of particles in this environment.

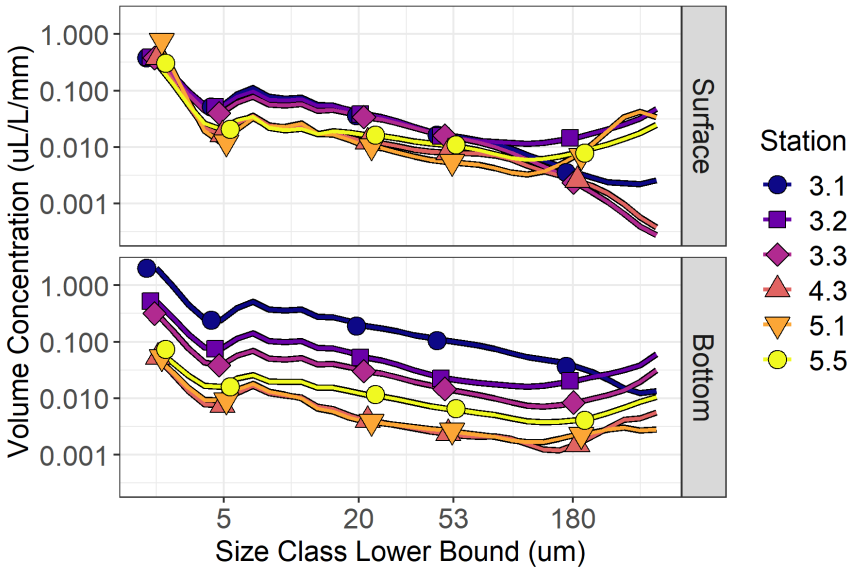

Title: The relationship between size, abundance, and mass of particles in the surface and bottom waters of the Chesapeake Bay

Authors:

Emily C. Dougherty,

University of Maryland Center for Environmental Science, Horn Point Laboratory

emilydougherty14@gmail.com, 610-705-2489

Jacob A. Cram,

University of Maryland Center for Environmental Science, Horn Point Laboratory

jcram@umces.edu, 410-221-8481

Ashley Hollins

University of Maryland Center for Environmental Science, Horn Point Laboratory

ahollins@umces.edu

Acknowledgments

The authors thank the MD Sea Grant REU program for supporting E.C.D during the sample collection phase of this project, as well as University of Maryland Center for Environmental Science for supplying J.A.C with start-up funds and ship time to complete this research. The authors thank M. Reynolds for assistance in field collection, S. Malkin and C. Fuchsman for coordinating field sampling efforts, L. Sanford for teaching us how to use the LISST and for helpful suggestions on analysis and writing, as well as the captain and crew of the R.V. Rachael Carson.

Abstract

Particulate matter modulates the transport of carbon and nutrients through estuarine environments. In the Chesapeake Bay, sinking of particles and their consumption by microbes likely modulates the emergence of a seasonal oxygen deficient zone. The relationship between particle size and abundance affects the transport dynamics of the particles and the biology of associated organisms. The variability of particle characteristics has not previously been characterized across the length of the Chesapeake Bay, nor has it been compared to the oxygen deficient zone. Therefore, we measured the size to mass and size to abundance relationship of suspended particles along the Chesapeake Bay during a major deoxygenation event. A laser scattering instrument measured particle size and abundance at six stations. Five particle size classes were sampled at surface and bottom depths. Particles in the less saline northern end of the Bay were less massive relative to size than particles farther south. Estimates of total particle mass, calculated by combining particle size to mass and particle size to abundance data, suggested that the anoxic region has lower particulate mass than overlying oxic water, perhaps because stratified water above the oxygen minimum zone keeps particles from the productive top layer from mixing into this region. Total particle mass was higher just above the sediment, suggesting resuspension of benthic particles. Our data provide the first systematic survey of size resolved particle abundances across the Chesapeake Bay oxygen minimum zone and provide context to future work in evaluating the biogeochemical role of particles in this environment.

Keywords: particles, particle size distribution, Chesapeake Bay, anoxia

Introduction

Particulate Matter (PM) is comprised of both organic (Particulate Organic Matter -- POM) and inorganic components and is an essential part of carbon transport in estuarine environments. Estuaries facilitate and regulate the transport of PM, as well as dissolved carbon, from rivers into the oceans (Fisher et al. 1998; Loh et al. 2006) and produce PM *in situ* (Savoye et al. 2011; Middelburg and Herman 2007). The dynamic conditions of estuaries create gradients in the abundance and composition of particles, which vary over spans of hours, seasons, or years (Canuel and Zimmerman 1999) and between locations (Fisher et al. 1998).

The concentration, size distribution, and dynamics (including aggregation and disaggregation) of PM in estuaries is affected by factors including turbulence, differential settling, Brownian motion, salinity gradients, and compounds produced by organisms that cause particles to aggregate (Eisma et al. 1991). High collision frequency, which depends on the concentration of particles and the energy of the water, can lead to particle aggregation, while turbulence breaks up particles (Fugate and Friedrichs 2003). Near the surface, particle size may be limited by low collision frequency (Fugate and Friedrichs 2003). Aggregation and breakup together drive particle size distributions to an equilibrium distribution, which can vary regionally in response to variation in turbulence and other factors (Chen et al. 1994). Sinking speed also affects particle size distributions, with denser faster sinking particles leaving the pycnocline more quickly than less dense slowly sinking or non-sinking particles (Fugate and Friedrichs 2003). PM that reaches the lower water column of estuaries settles into the bed, where strong turbulence may cause re-suspension of large particles and more breakup (Hill et al. 2001).

The Chesapeake Bay is the largest estuary in the United States, with the main stem measuring 320 km (Schubel and Pritchard, 1986). Within the Bay, there are strong salinity gradients, with a low salinity region (< 0.5 ppt) in the northern section, a mesohaline zone (0.5 – 25 ppt) extending approximately from 39˚N latitude to the mouth of the Potomac River, and a high salinity region (> 25

ppt) near the mouth of the Bay (Maryland Department of the Environment). The Chesapeake Bay has an expanding region of seasonal anoxia (Testa 2018; Kemp 1992), with deficits occurring annually in the mesohaline region (Officer et al. 1984). Deoxygenation is driven by microbes at depth consuming the organic portion of particles that originate in high production surface waters (Robinson 2019). In the Chesapeake Bay, these particles originate from surface waters primarily in the mainstem of the Bay (Wang and Hood 2021). Anoxic regions are intensified by sewage and agricultural runoff, which increase the rate of phytoplankton production (Canuel and Zimmerman 1999).

Since the Chesapeake Bay is a region of high biological productivity and diverse habitats, there is high variability in the origin and distribution of PM. The balance of aggregation, disaggregation, and particle transport differ between the mouth of the Bay, the seasonally anoxic mesohaline, and the Upper Bay. Several studies have characterized particle size distributions near the mouth of the Bay: One of these studies combined acoustic and optical measurements of particle properties and identified temporal variability in the sinking speed and size properties of particles near the mouth of the Bay (Fugate and Friedrichs 2002). In another site in the lower Bay, it was found that higher turbulent kinetic energy near the bed is associated with larger particle sizes (Fugate and Friedrichs 2003). This result contrasted with other estuarine river environments in this study, where turbulence near the riverbed fragments particles, keeping their sizes small. The authors suggested that the Chesapeake Bay has a biologically active benthic community, which produce compounds that create large aggregate particles under turbulent conditions (Fugate and Friedrichs 2003).

No study, to our knowledge, has characterized the particle size distribution spectrum in the mesohaline region of the Bay. However, several studies have explored the origin of particles contributing to the seasonally anoxic region of the Bay. Particle transport into the mesohaline is driven in large part by advection of deep water from the high salinity mouth of the Bay and particle sinking (Jonas 1992). Particle tracking experiments have shown that particles that ultimately sink into the

anoxic region of the Bay vary in their origin depending on the tidal cycles and corresponding currents (Wang and Hood 2021). The organic portion of this particulate matter has been shown to degrade quickly (Jonas and Tuttle 1990), and so fuels the oxygen removal in this anoxic region.

In the Upper Bay, there is a defined estuarine turbidity maximum (ETM) region, where the Susquehanna River meets the more brackish waters of the main Bay (Schubel and Biggs 1969). The ETM is caused by suspension and entrainment of sediment from the bay floor, which is maintained by interactions between tidal forces and the steep salinity gradient (Sanford et al. 2001). This region is characterized by vertical stratification and seasonal variability in particle concentrations (Fisher et al. 1998). Particle concentrations are influenced by particles coming from the Susquehanna River, particularly in spring when there is more runoff into the river (Schubel and Biggs 1969). Total particle concentrations in the upper Bay are generally higher than in the mesohaline region (Biggs 1969).

While each of these studies examined particle distributions at specific regions and sites in the Chesapeake Bay, no previous study has, to our knowledge, characterized particle size distribution across the length of the Bay. While comparing the different papers can give us insight about differences between these regions, they each use different measurements and are taken at different times. Furthermore, no study to our knowledge has examined particle size distributions within, around and above the oxygen deficient zone. Therefore, in this study we carried out measurements of the particle size to abundance distribution and size to mass distribution along the surface and bottom of the mainstem of the Bay, from the high salinity mouth of the Bay to the lower salinity waters just below the ETM. Such data will provide information about the processes that shape particle size and transport. In particular, we are interested in how the anoxic zone affects particle dynamics, because particles attenuate slowly in anoxic regions (Rasse and Dall'Olmo 2019). Exploring the interactions between anoxic environments and particle size distributions has the potential to provide clues about how hypoxia relates to the regional carbon cycle.

Methods

Samples and observations were collected July 22, 23, and 24, 2019, on the R/V *Rachel Carson* from six stations along the main stem of the Chesapeake Bay, corresponding to the Maryland Department of the Environment's water quality monitoring stations CB3.1 (39.24°N,76.24°W, corresponding to 13.3m water column depth), CB3.2 (39.16°N, 76.30 °W, 12.2 m), CB3.3C (39.00°N, 76.36°W, 24.1 m), CB4.3C (38.56°N, 76.43°W, 27.1 m), CB5.1 (38.32°N, 76.29°W, 34.3 m), and CB5.5 (37.69°N, 76.19°W, 17.7 m) (Fig. 1A).

A Seabird CTD (Conductivity, Temperature, and Depth), mounted on the CTD-rosette measured water Temperature, Salinity, Fluorescence, and pH throughout the water column. At each station, a laser *in-situ* scattering and transmissometry (LISST-100X) instrument (Sequoia Scientific, Inc.) was lowered into the water to measure a vertical profile of the particle size distribution spectrum. The LISST uses the laser light diffracted by particles to provide a reading of the total volume concentration (µL Particles/L Water) of particles in several bins, each represented by a minimum particle diameter (LISST 100X Manual 2015). Particles were assumed to be spherical in shape, so the diameters were used to calculate the average volume of an individual particle in each bin. From the total volume sampled and the individual particle volumes, the number of particles per liter of water was calculated for each size bin. For purposes of comparison to particle mass measurements, the LISST size data were grouped into the filter size fractions of 1.2 µm, 5 µm, 20 µm, 53 µm, and 180 µm, each corresponding to our filter size fractions, by summing particle abundances of all LISST size bins that fell within each filter size bin. No particle number was obtained for the 0.2 µm filter size, since this size is below the LISST detection threshold of 1 µm. Similarly, LISST measurements were not recorded for the 500 µm size fraction as we found measurements above 200 µm to be inconsistent. Initial data processing was carried out by the proprietary LISST-SOP software provided for the LISST-100X by Sequoia scientific.

All subsequent data analysis was performed in the R statistical programming language (R Core Team 2019).

Water samples were collected in the surface mixed layer and five meters above the floor of the Bay at each station. At station 4.3C a sample was also taken at the oxycline in the mid water column (Fig. 1). For each sample, between 13 and 20 liters of water were collected with Niskin bottles and gravity filtered, in sequence, through five nylon filters with diameters of 150 cm and decreasing pore sizes of 500 um, 180 µm, 53 µm, 20 µm, and 5 µm. Each filter was rinsed with 0.2 µm filtered seawater from the same station. An aliquot of this rinse water was vacuum filtered through a pre-weighed 25 mm diameter 1.2 µm pore size glass fiber filter (Whatman 16936209) and was saved for analysis of particle mass.

In the lab, particle mass was measured for each size fraction by drying and re-weighing the pre-weighed glass fiber filters and calculating its change in mass. This value was divided by the number of particles corresponding to this size bin to find the average mass per particle in each size class.

The slope and intercept of the particle size to abundance relationship and size to mass relationship were calculated on the log of the values of particle size, abundance and mass. The slope of the size to abundance relationship is called the particle size distribution slope (Jackson et al. 1997), and the slope of the size to mass relationship is the particle fractal dimension (Jackson et al. 1997). Intercepts correspond to the predicted abundance and mass of 1 µm particles. Total particle mass profiles throughout the water column were estimated by multiplying particle abundances in each size class, measured by the LISST, by the empirically derived size to mass relationships determined by the filtration method. Data from the top meter of the water column was removed from the plots for particle mass and abundance profiles, as light from the surface is known to create artifactually high estimates of particle abundance in these samples (L. Sanford pers. Comm.).

Results

Physics and Chemistry of the Bay

Stations followed a salinity gradient, with the lower salinity associated with northern stations near the mouth of the Susquehanna River and higher salinity with stations closer to the mouth of the Bay (Fig. 1A-B). While station 3.1 was fully mixed, all remaining stations had an oxygenated mixed layer, followed by a pycnocline, below which water was cooler and more saline (Fig. 1B, C, F). All stations except 3.1 and 5.5 were anoxic below the pycnocline. The deepest samples at station 4.3 and 5.1 were sulfidic, as evidenced by a sulfurous smell to the water (M. Gomes Pers. Comm.). Chlorophyll fluorescence was present at all stations through the pycnocline (Fig. 1D). pH was lower in the two upper-most stations than in the others (Fig. 1E).

Total Particle Abundances

The LISST detected on the order of 10^8 particles per liter at most stations through most of the water column (Fig. 2). At most stations, there was an increase in particle abundance, usually to around 10^9 particles per liter, just above the floor of the Bay. In the anoxic water, particle abundance was generally lower, often around 10^7 particles per liter. There were regions of apparently very low particle numbers in the oxycline, in stations where an oxycline was present (Fig. 2). A general additive model of form `gam(Total_Particles ~ s(Pressure) + s(pressure, by – as.factor(Station))` indicated that across all stations, this variability with depth was statistically detectable, and that there was statistically significant station to station variability ($R^2 = 0.78$ (overall model), $p < 0.001$ (for all interaction terms but one (pressure * station 3.3))). Particle abundance normalized to LISST size bins decreased as particle size increased (Fig. 3).

Particle Size to Abundance Relationship

At all stations, there was a negative power law relationship between particle size and particle abundance. The slope of the power law distribution, which is the slope of the relationship between log

transformed particle abundance and log transformed particle size, ranged at most stations and depths from -3.5 to -4. However, several depths at some stations had anomalously large negative particle size distribution slopes (Fig. 4). A general additive model `gam(Particle_Size_Distribution_Slope ~ s(Pressure) + s(pressure, by – as.factor(Station))`, suggested that that there was statistically significant variability in the particle size distribution between depths, and that this relationship varied between stations ($R^2 = 0.167$, $p < 0.01$).

Total Particle Mass Patterns

Estimated total particle mass per liter of all particles > 1.2 μm ranged from 10 to 100 mg /L (Fig. 5). Calculated particulate matter concentrations were higher in the bottom sample than the surface sample at every station except 4.3 (OLS log(Mass) ~ Depth [Surface or Bottom, excludes Oxycline], F = 7.6, $p = 0.02$). At station 4.3 the sample taken in the oxycline had highest biomass, followed by the surface sample, and then the bottom sample. Particulate matter concentrations estimated by LISST measurements were generally higher in the surface than in the bottom, except at stations 3.1 and 3.2. There was no detectable relationship between station latitude and observed particle mass (Ordinary Least Squares regression of form `log(Mass) ~ Latitude`; F = 0.001, $p = 0.97$).

Particle Mass to Size Relationship

Mass per particle increased with particle size, following a power law (Fig. 6). The masses of particles of each size class were similar at each depth, ranging from about 10^{-9} mg/particle in the 1.2 μm class to about 10^{-3} mg/particle in the 500 μm class. There did not appear to be statistically significant differences between the slopes of the relationship between particle size and particle mass (Fig. 6). A linear model of form `ln(Mass) ~ ln(Size) * Station * Depth`, where "ln" indicates the natural logarithm function, found that while there was a relationship between size and mass ($p < 10^{-10}$), neither station, depth, nor any interaction between size, station and or depth had any statistically significant relationship to particle mass. However, a linear model of form `ln(Mass) ~ ln(Size) +

Station` suggested that there was station to station variability in the intercept of the size to mass relationship ($p < 0.01$ for all stations, with the exception of stations 3.2 and 3.1 which had statistically identical intercepts). The `eemeans` package was used to compare the y intercepts of the size to mass relationship at each station. It was found that station 3.1 had statistically significantly lighter particles, adjusted for size, than stations 4.3 (difference = -2.5 +- 0.7 (1 standard error) log(mg/Particle), t-ratio = -3.86, $p = 0.012$) or 5.1 ($p = 2.5$ +/- 0.7 log(mg/Particle), t-ratio = -3.79, $p = 0.014$). All other differences were found to be not statistically significant, after adjusting for multiple comparisons (FDR < 0.05). (Fig. 7).

Calculated Total Particle Mass Profiles

By combining the information from the mean particle size to mass relationship with the abundances of particles at each size, we were able to calculate expected particle mass throughout the water column at each station (Fig. 5; black circles). A general additive model of form `gam(Total_Particle_Mass ~ s(Pressure) + s(pressure, by = Station))` suggested that particle mass varied statistically significantly between depths($F = 9.4$, $p < 10^{-10}$), with all stations except 3.3 and 5.5 showing statistically significant deviations from the main profile ($F >= 3.1$ $p <0.003$ for all remaining stations). Calculated total particle mass appeared to be related to, but was often an underestimate of, observed total particle mass (Fig. 5).

Discussion

Measurements of physical and chemical parameters (Fig. 1) showed depth profiles typical of previous measurements of the Chesapeake Bay at this time of year (Pritchard 1952; Murphy et al. 2011). The location of the stations arranged along the length of the Bay allowed for gradients to be observed. The salinity gradient in the Chesapeake is formed as colder, denser saline water enters the mouth of the Bay and flows northward, while warmer, less dense, freshwater enters from rivers and tributaries and moves south (Pritchard 1952). The density difference in these two layers forms a

pycnocline, which was observed at all stations. The pycnocline blocks the vertical transfer of oxygen, creating the anoxic zones that were seen in most stations. Large anoxic and hypoxic zones form during summer in the Chesapeake Bay and were clearly seen in July when measurements were taken. Anoxic bottom waters have been shown to lead to increases in sulfide concentrations (Roden and Tuttle 1992), as seen in the sulfidic samples collected in stations 4.3 and 5.1.

Throughout the Chesapeake Bay, particle size distribution profiles displayed a power law relationship between size and abundance, with slope usually between -3.5 and -4, which is within the range of values seen in open ocean locations (Sheldon et al. 1972; Kostadinov et al. 2009; Cram et al. 2018). The slopes generally did not show much change with depth. This pattern is consistent with the findings of a study that size distribution does not change significantly with depth across the Atlantic Ocean (Gordon 1970), though it contrasts with measurements of an oxygen deficient zone in the Eastern Tropical North Pacific that found changes in the particle size slope with depth (Cram et al. 2021). While particle size spectra have been measured in the Chesapeake Bay, the particle size distribution slope is often not reported (Schubel 1968; Schubel and Nelson 1973). The anomalous spikes of particularly negative slopes, seen especially in stations 4.3, 5.1, and 5.5, could indicate a lack of large particles in the oxycline, as the spikes occurred at approximately the same depth. These spikes could also be artifacts, perhaps induced by changes in salinity or temperature or introduced by the LISST's electronics.

The particle size to mass relationship also stayed consistent throughout stations and depths, with mass increasing and density decreasing in larger particles. The slopes of the size to mass relationship, or fractal dimension, at each station and sample depth were similar to the values calculated in other particle studies. For instance, Fall et al. (2021) calculated fractal dimension in the York River as the size to density relationship with a bulk value of 2.25. Other studies have quantified fractal dimensions from the size to density or size to settling velocity relationship in the Chesapeake

Bay (Sanford et al. 2004) and other estuaries and marine environments (Hill et al. 1998; Guidi et al. 2008; Jackson et al. 1997). These previous measurements of fractal dimension values for particles typically fall somewhere between 1.3 and 2.5, and the values for this study are on the low end of that range. Aggregation and disaggregation of particles affect their fractal dimension, with larger aggregates having lower fractal dimensions than small particles. Li and Logan (1995) found fractal dimension to decrease from 2.49 to 1.68 as particles coagulated during a phytoplankton bloom. It is possible that collection methods in this study could lead to disaggregation of particles; however, the fractal dimensions' consistency with other studies lend confidence to our observations.

Although particle size to mass relationships stayed consistent across stations and depth, total particle abundance and mass both varied by depth. Particle abundance profiles generally tracked total particle mass profiles (Fig. 2 and 5). The calculated total mass values from collected particles were consistently higher than the estimated mass based on LISST measurements, especially in station 4.3 (Fig. 5). This disparity could be caused by the assumption that the power law relationship between size and mass is the same at each station. Particle abundance and total particle mass both increased near the bottom of the water column, suggesting that the current is resuspending sediment from the floor of the Bay. In the anoxic water below the pycnocline, particle abundance and total mass was lower than in surface waters, suggesting either lower production of particles in this region or faster removal. This effect may occur when the pycnocline separates anoxic water from the more productive surface waters, which prevents particles that primarily form in the surface from mixing into the anoxic waters. This scarcity of particle mass below the pycnocline suggests either low transport or fast removal of particles into this region. We argue that since particle remineralization is thought to be slow in anoxic water (Cram et al. 2018), it is likely the former process, low *in situ* production and low flux from the surface that leads to the lower anoxic particle mass. Particle abundance and particle mass profiles diverged near the middle of the depth profiles, where abundance sharply decreased in most stations, but mass did not.

This result could suggest that the decreases in particle abundance were generally among small particles that had less impact on biomass, although the size distribution slopes in some stations suggest that small particles were still more abundant relative to large particles in the oxycline. The sharp decreases in particle abundance could also be the same artifacts that may be seen in the particle distribution slopes.

This study was the first characterization of particle size to abundance and size to mass distribution across the length of the Chesapeake Bay as well as with depth. Overall, there was little variation by latitude, with particle size, abundance, and mass mostly following the same patterns at each station. Although the Bay covers a large area and sample stations varied in proximity to the Susquehanna River and the mouth of the Bay, the results suggest that factors other than latitude lead to a variability of particle characteristics. Significant differences were observed vertically, with particle mass and abundance higher just above the floor and low in the body of the anoxic layer. This low total particle mass in the anoxic water suggests that particles from the photic zone are not mixing into the anoxic water, and also that particle sinking flux happens on either a slower or similar time scale to carbon removal, either by carbon settling into the sediment or by remineralization. The low particle abundances could indicate the presence of particle remineralization despite the lack of oxygen, because if remineralization was absent, we would expect carbon accumulation in this region even if particle flux into the region was low. The mass of particles also suggests low input of carbon into this region, suggesting carbon limitation of microorganisms in the anoxic region.

Conclusion

This analysis of particulate organic matter provides data for particle size distribution and particle mass at surface and bottom depths across various stations in the mesohaline region of the Chesapeake Bay. This study was the first to analyze particle distribution at multiple locations in the Bay, with samples collected at the same time. Generally, particle size/abundance and size/mass

relationships were similar between stations and depths. Particle abundance and mass mostly followed similar patterns to each other, decreasing in the anoxic zones, with an increase near the bottom of the Bay. The results show the influence of depth on particle distribution, while patterns stayed consistent throughout station latitudes at the time of sample collection in July.

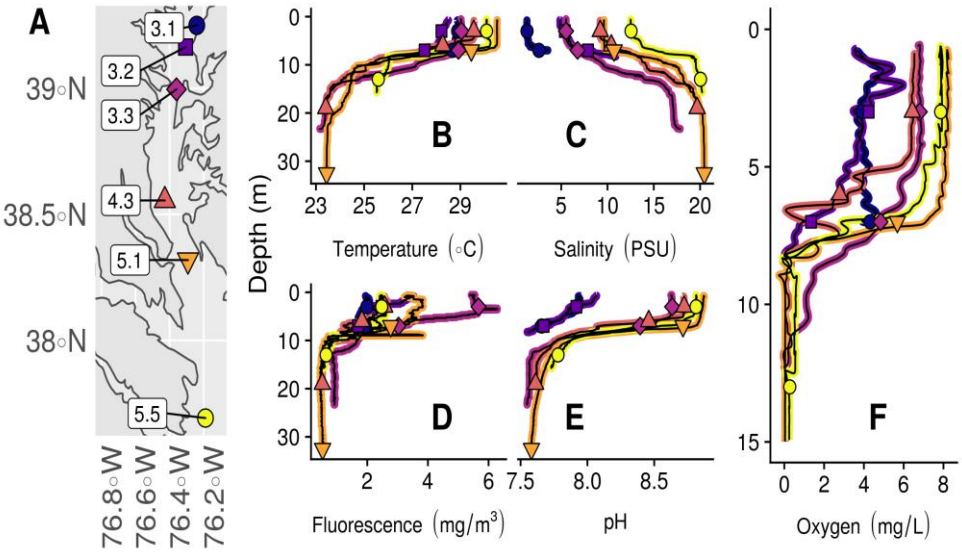

Fig. 1 Sample Collection locations (A) and corresponding oceanographic data (B-F) measured by a seabird CTD**.** These included Temperature (A), Salinity (B), Fluorescence (D), pH (E), and oxygen (F). Shapes in the CTD profiles indicate the locations where particle samples were collected. Lines indicate the corresponding CTD profiles. All stations have two samples, one in the upper mixed layer, and one below, except station 4.3 which also has a sample taken at the oxycline. CTD profiles all extend from the surface to approximately 5 m above the seafloor, except station 5.5, which only extended to 15 m

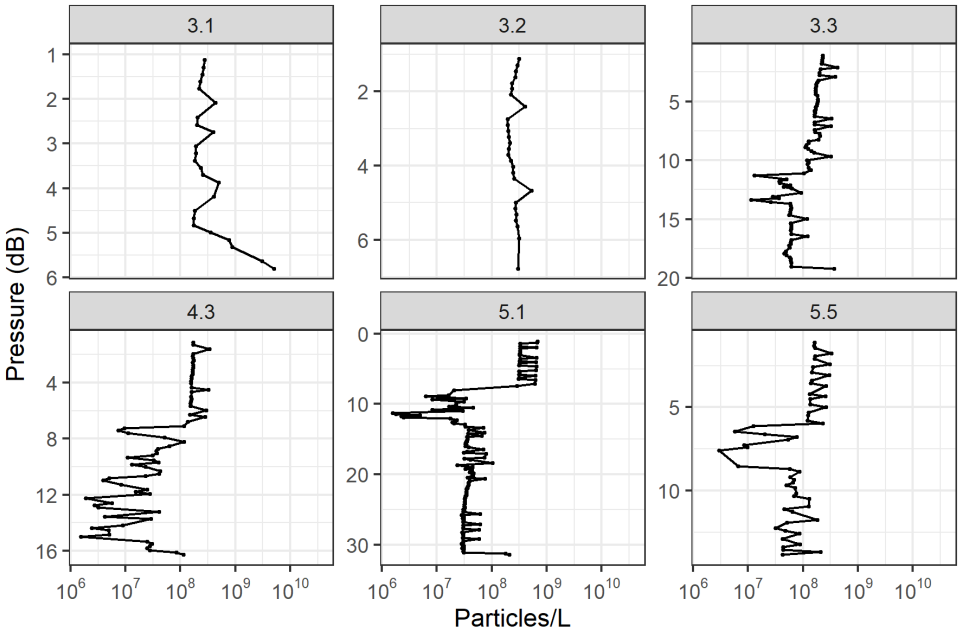

Fig. 2 Particle Abundance. The number of particles per liter of water throughout the water column, as estimated by the LISST. The y axis indicates pressure in dB. The x axis is on a log scale and indicates total particles per liter

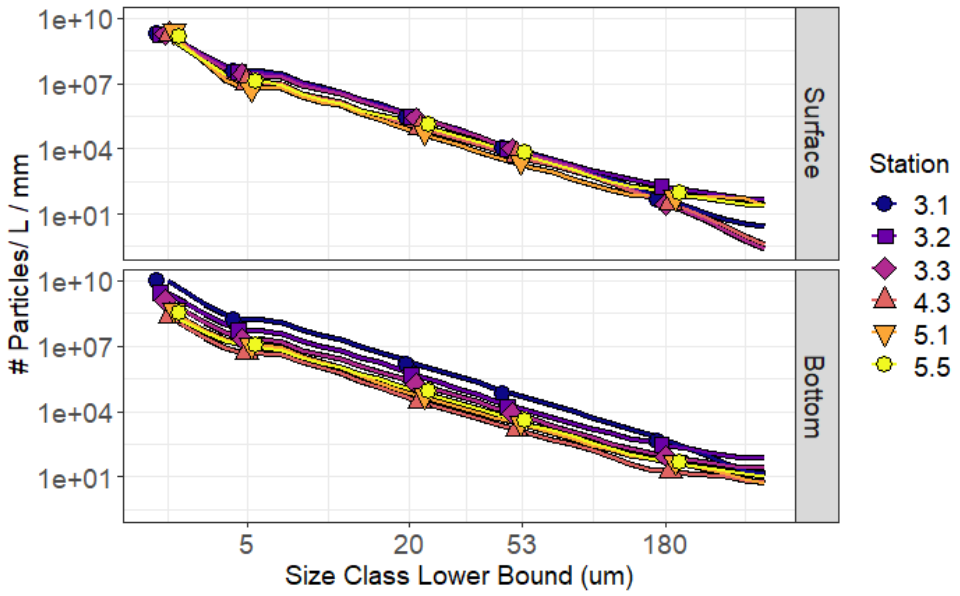

Fig. 3 Particle Abundance at Sample Depths. The number of particles per liter of water per particle size (x axis) for all size bins provided by the LISST (y axis), shown only for the surface and bottom depths where particle samples were collected. Points are where the LISST size bins most closely match the sizes of the filters that were used for particle collection

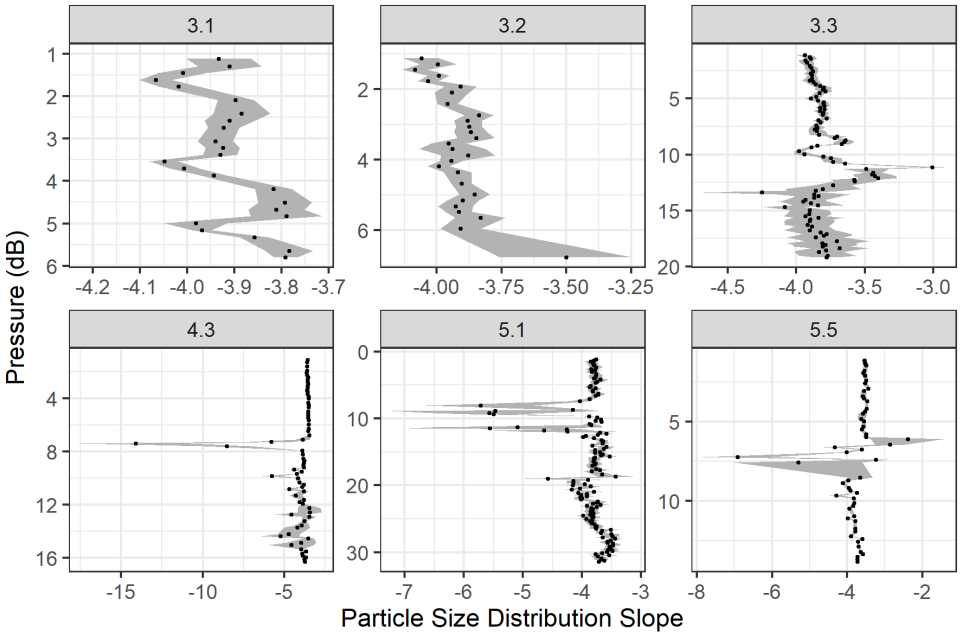

Fig. 4 Particle size distribution slopes (x axis) indicate the slope of the relationship between log transformed particle size and log transformed particle abundance. More negative values indicate a higher relative proportion of small particles and a smaller relative proportion of large particles

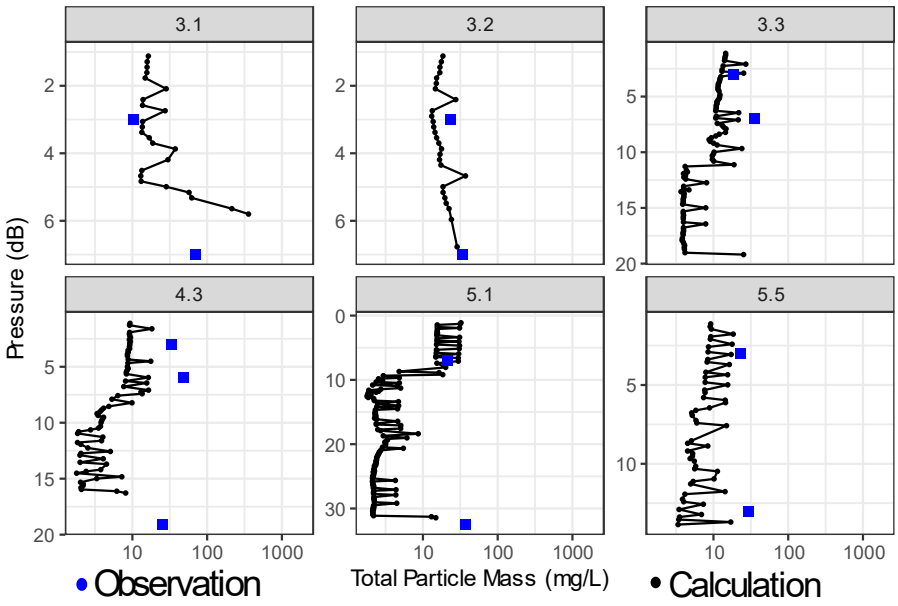

Fig. 5 Blue squares – Total particle mass collated at each station. Total Observed Particulate mass was determined by summing over all size fractions and includes both organic and inorganic matter. Black circles – Total calculated particle mass was estimated by multiplying LISST measurements of size specific particle abundances by size specific particle mass estimates

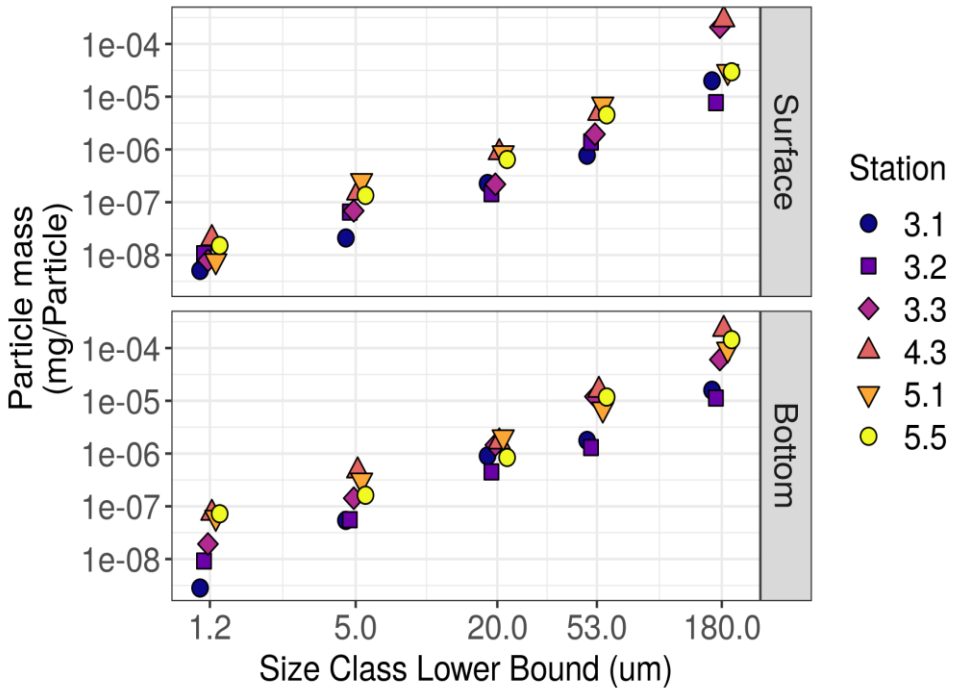

418

419 **Fig. 6** Mass per Particle. The mass of the total particles collected on each size filter normalized to

420 particle abundance. Mass was calculated for each particle size using the diameters on the lower bound

421 of each size bin. These results are virtually the same as when calculated with the geometric mean of

422 each bin, suggesting that most particles are on the low end of their bin size range

423

424

425

426

427

428

429

430

431

432

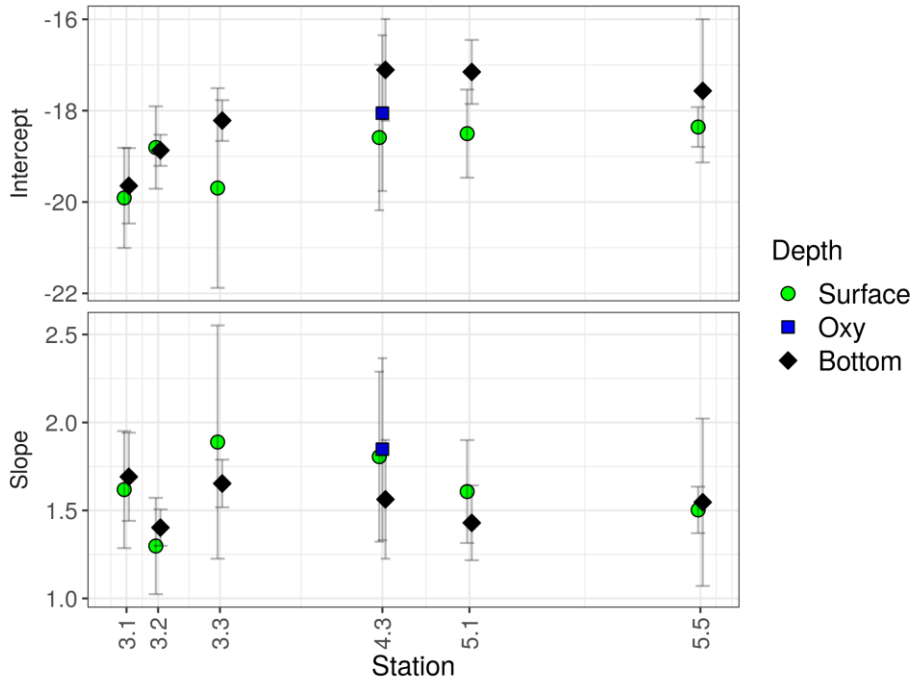

Fig. 7 The intercepts (natural log of the predicted mass of particles 1 μm in size) and slope of the mass to size relationship depicted in Figure 6. Confidence intervals indicate 2 standard errors

448 **References**

449 Biggs, R.B. 1969. Sources and distribution of suspended sediment in northern Chesapeake Bay. *Marine*
450 *Geology.* 9: 187-201.

451 Canuel, E.A. and A.R. Zimmerman. 1999. Composition of particulate organic matter in the southern
452 Chesapeake Bay: sources and reactivity. *Estuaries*. 22(4): 980-994.

453 Chen S., D. Eisma, and J. Kalf. 1994. In situ size distribution of suspended matter during the tidal cycle
454 in the Elbe Estuary. *Netherlands Journal of Sea Research*. 32(1): 37-48.

455 Cram J., C. Fuchsman, M. Duffy, J. Pretty, R. Lekanoff, J. Neibauer, et al. 2021. Slow particle
456 remineralization, rather than suppressed disaggregation, drives efficient flux transfer through
457 the Eastern Tropical North Pacific Oxygen Deficient Zone (preprint). *Oceanography*.

458 Cram, J.A., T. Weber, S.W. Leung, A.M.P. McDonnell, J.H. Liang, C. Deutsch. 2018. The role of
459 particle size, ballast, temperature, and oxygen in the sinking flux to the deep sea. *Global*
460 *Biogeochemical Cycles.* 32: 858-876.

461 Eisma, D. 1991. Particle size of suspended matter in estuaries. *Geo-Marine Letters*. 11(3): 147-153.

462 Fall K.A., C.T. Friedrichs, G.M. Massey, D.G. Bowers, and S.J. Smith. 2021. The importance of
463 organic content to fractal floc properties in estuarine surface waters: Insights from video,
464 LISST, and pump sampling. *Journal of Geophysical Research: Oceans*. 126. e2020JC016787.

465 Fisher T.R., J.D. Hagy, and E. Rochelle-Newall. 1998. Dissolved and particulate organic carbon in
466 Chesapeake Bay. *Estuaries*. 21(2): 215.

467 Fugate, D.C. and C.T. Friedrichs. 2002. Determining concentration and fall velocity of estuarine
468 particle populations using ADV, OBS, and LISST. *Continental Shelf Research*. 22: 1867-1886.

469 Fugate, D.C. and C.T. Friedrichs. 2003. Controls on suspended aggregate size in partially mixed
470 estuaries. *Estuarine, Coastal and Shelf Science*. 58(2): 389-404.

471 Gordon, D.C. 1970. A microscopic study of organic particles in the North Atlantic Ocean. *Deep-Sea*
472 *Research*. 17: 175-185.
473 Guidi L., G.A. Jackson, L. Stemmann, J.C. Miquel, M. Picheral, and G. Gorsky. 2008. Relationship
474 between particle size distribution and flux in the mesopelagic zone. *Deep-Sea Research I.* 55:
475 1364-1374.
476 Hill P.S., J.P. Syvitski, E.A. Cowan, and R.D. Powell. 1998. In situ observations of floc settling
477 velocities in Glacier Bay, Alaska. *Marine Geology*. 145: 85-94.
478 Hill P.S., G. Voulgaris, and J.H. Trowbridge. 2001. Controls on floc size in a continental shelf bottom
479 layer. *Journal of Geophysical Research*. 106(C5): 9543-9549.
480 Jackson G.A., R. Maffione, D.K. Costello, A.L. Alldredge, B.E. Logan, and H.G. Dam. 1997. Particle
481 size spectra between 1 μm and 1 cm at Monterey Bay determined using multiple instruments.
482 *Deep Sea Research Part I: Oceanographic Research Papers*. 44(11): 1739–1767.
483 Jonas, R.B. 1992. Microbial processes, organic matter and oxygen demand in the water column, p. 113-
484 148. In D. E. Smith, M. Leffler, and G. Mackiernan (eds.), Oxygen Dynamics in the
485 Chesapeake Bay: A Synthesis of Recent Research. Maryland Sea Grant, College Park,
486 Maryland.
487 Jonas, R.B. and J.H. Tuttle. 1990. Bacterioplankton and organic carbon dynamics in the lower
488 mesohaline Chesapeake Bay. *Appl. Environ. Microbiol*. 56(3): 747-757.
489 Kemp W., P. Sampou, J. Garber, J. Tuttle, and W. Boynton. 1992. Seasonal depletion of oxygen from
490 bottom waters of Chesapeake Bay: roles of benthic and planktonic respiration and physical
491 exchange processes. *Marine Ecology Progress Series*. 85: 137–152.
492 Kostadinov T.S., D.A. Siegel, and S. Maritorena. 2009. Retrieval of the particle size distribution from
493 satellite ocean color observations. *Journal of Geophysical Research (Oceans).* 114: C09015.
494 LISST-100X Particle Size Analyzer User's Manual. 2015. *Sequoia Scientific, Inc*. Version 5.1.

Li, X. and B.E. Logan. 1995. Size distributions and fractal properties of particles during a simulated phytoplankton bloom in a mesocosm. *Deep Sea Research Part II: Topical Studies in Oceanography.* 42(1): 125-138.

Loh A.N., J.E. Bauer, and E.A. Canuel. 2006. Dissolved and particulate organic matter source-age characterization in the upper and lower Chesapeake Bay: a combined isotope and biochemical approach. *Limnology and Oceanography*. 51(3): 1421-1431.

Middelburg, J.J. and P.M.J Herman. 2007. Organic matter processing in tidal estuaries. *Marine Chemistry.* 106(1-2): 127-147.

Murphy R.R., W.M. Kemp, and W.P. Ball. 2011. Long-Term Trends in Chesapeake Bay Seasonal Hypoxia, Stratification, and Nutrient Loading. *Estuaries and Coasts.* 34: 1293-1309.

Officer C.B., R.B. Biggs, J.L. Taft, L.E. Cronin, M.A. Tyler, and W.R. Boynton. 1984. Chesapeake Bay anoxia: origin, development, significance. *Science*. 223: 22-27.

Pritchard, D.W. 1952. Salinity distribution and circulation in the Chesapeake Bay estuarine system. *Journal of Marine Research*. 11: 106-123.

R Core Team. 2019. R: A language and environment for statistical computing. R Foundation for Statistical Computing, Vienna, Austria. URL https://www.R-project.org/.

Rasse, R. and G. Dall'Olmo. 2019. Do Oceanic Hypoxic Regions Act as Barriers for Sinking Particles? A Case Study in the Eastern Tropical North Atlantic. *Global Biogeochemical Cycles*. 33(12): 1611-1630.

Robinson, C. 2019. Microbial Respiration, the Engine of Ocean Deoxygenation. *Frontiers in Marine Science*. 5: 533.

Roden, E.E. and J.H. Tuttle. 1992. Sulfide release from estuarine sediments underlying anoxic bottom water. *Limnology and Oceanography*. 37: 725–738.

518 Sanford L.P., P.J. Dickhudt, L. Rubiano-Gomez, M. Yates, S.E. Suttles, C.T. Friedrichs, D.D. Fugate,
519 and H. Romine. 2004. Variability of Suspended Particle Concentrations, Sizes, and Settling
520 Velocities in the Chesapeake Bay Turbidity Maximum. In *Flocculation in Natural and*
521 *Engineered Environmental Systems*, ed. I.G. Droppo, G.G. Leppard, S.N. Liss, and T.G.
522 Milligan, 211-236. Boca Raton: CRC Press.
523 Sanford L.P., S.E. Suttles, and J.P. Halka. 2001. Reconsidering the physics of the Chesapeake Bay
524 estuarine turbidity maximum. *Estuaries*. 24(5): 655–669.
525 Savoye N., V. David, F. Morisseau, H. Etcheber, G. Abril, I. Billy, K. Charlier, G. Oggian, H.
526 Derriennic, and B. Sautour. 2011. Origin and composition of particulate organic matter in a
527 macrotidal turbid estuary: The Gironde Estuary, France. *Estuarine, Coastal and Shelf Science.*
528 108(2012): 16-28.
529 Sheldon R.W., A. Prakash, and W.H. Sutcliffe. 1972. The size distribution of particles in the ocean.
530 *Limnology and Oceanography*. 27(3): 327-340.
531 Schubel, J.R. 1968. Turbidity maximum of the northern Chesapeake Bay. *Science*. 161(3845): 1013–
532 1015.
533 Schubel, J.R. and R.B. Biggs. 1969. Distribution of seston in upper Chesapeake Bay. *Chesapeake*
534 *Science.* 10(1): 18-23.
535 Schubel, J.R. and B.W. Nelson. 1973. Distribution and Transportation of Suspended Sediment in the
536 Upper Chesapeake Bay. In Environmental Framework of Coastal Plain Estuaries. *Geological*
537 *Society of America Memoirs.* 133: 151-167.
538 Schubel, J.R. and D.W. Pritchard. 1986. Responses of upper Chesapeake Bay to variations in discharge
539 of the Susquehanna River. *Estuaries.* 9: 236-249.
540 Testa, J.M., W.M. Kemp, and W.R. Boynton. 2018. Season-specific trends and linkages of nitrogen and
541 oxygen cycles in Chesapeake Bay. *Limnology and Oceanography*. 63: 2045-2064.

542 Wang, J. and R.R. Hood. 2021. Modeling the Origin of the Particulate Organic Matter Flux to the
543 Hypoxic Zone of Chesapeake Bay in Early Summer. *Estuaries and Coasts.* 44: 672-688.

Supplemental Tables

Table S1. CTD profiles of each station. Station corresponds to Maryland Department of the Environment CB central stations. For instance, 4.3 corresponds to MDE station CB4.3C. Depth (m) is estimated from a pressure sensor, assuming every m corresponds to one dB of pressure. Sensor describes the measurement type with units as follows: Oxygen (mg/L), Temperature (°C), Salinity (PSU), Fluorescence (mg/m^3), PAR ($umol/m^2/s$), and pH (unitless). Fluorescence sensors were not calibrated prior to this project, so values should be treated as relative fluorescence.

Table S2. LISST profiles and preliminary calculations. Station as in table S1. Pressure in dB, according to the LISST's built in sensor. Minutes+seconds – relative time measurement. goingdown – 1 if the LISST is descending. size – size bin, as recorded by the instrument. vc – volume concentration. Estimated particle volume in that bin, assuming spherical particles. VolumePerParticle – particle volume of a particle of diameter "size". number_of_particles – estimated from volume concentration assuming a spherical particle. Value is in particles/L.

Table S3. Estimates of total particle mass, and total particle abundance associated with our nylon filter size fractions. Station as in tables S1 and S2. Size_Class – lower bound of our filtration size class. For instance, 1.2 refers to all particles larger than 1.2 μm and smaller than 5 μm. Depth – is categorical. Sample_depth – the depth at which the measurement was taken. MassperLiter – measurement of particle mass in that size bin (mg/L). Calculated by comparing pre and post weights of a gff that had measured a known volume of water resuspended from a nylon filter.

ParticlesPerL – total number of particles, calculated by summing over all LISST bins within that size range (#/L).

Figure S1. Volume concentration data from the LISST. The particle volume concentration in µL/L/mm (x axis) for all size bins provided by the LISST (y axis), shown only for the surface and bottom depths where particle samples were collected. Points are where the LISST size bins most closely match the sizes of the filters that were used for particle collection.